Available online at www.easdprocedia.org
EASD Procedia EURODYN (2020) 3067-3078

EASD Procedia

EURODYN 2020
XI International Conference on Structural Dynamics
M. Papadrakakis, M. Fragiadakis, C. Papadimitriou (eds.)
Athens, Greece, 23–26 November 2020

SIMPLIFIED ESTIMATION OF DESIGN FAULT DISPLACEMENT FOR BURIED PIPELINES AT FAULT CROSSING

Vasileios E. Melissianos[1] and Dimitrios Vamvatsikos[2]

[1,2] Institute of Steel Structures, School of Civil Engineering, National Technical University of Athens
9, Iroon Polytechneiou str., GR-15780 Zografou Campus, Athens, Greece
e-mail: [1]melissia@mail.ntua.gr, [2]divamva@mail.ntua.gr

Keywords: pipeline – fault crossing, fault offset hazard, simplified expressions

Abstract. *A set of simplified expressions are derived for estimating the design fault displacement for pipelines crossing active faults by considering alternative scenarios, seismicity levels, and the pertinent uncertainties. Buried steel pipelines are an efficient and safe means of oil and gas onshore transportation and provide a direct link between extraction, processing, and consumption of fuel. Hazardous materials are transported via pipelines and consequently, any pipe failure may have devastating consequences. In case of crossing an active tectonic fault, the pipeline may be subject to significant deformations and strains threatening its integrity in the event of an earthquake. Its design hinges on a single value of the fault displacement magnitude, typically estimated as a specific "safe" percentile (e.g., 84%) from the surface displacement distribution given a "maximum" magnitude, estimated from regression models parameterized on fault characteristics. This single-scenario-based approach can lead to either conservative or unconservative designs as the actual level of safety is unknown. Instead, Probabilistic Fault Displacement Hazard Analysis (PFDHA) can provide a robust probabilistic basis to determine design values corresponding to specified return periods, at the cost of requiring extensive seismological data that may be unavailable for every single major or minor fault that a transmission or distribution pipeline crosses. Herein, logic tree aggregation is employed to cater to different levels of data completeness and provide design-level fault displacement values that incorporate all pertinent uncertainties.*

ISSN:2311-9020
Peer-review under responsibility of the Organizing Committee of EURODYN 2020.
doi: 10.47964/1120.9250.19632

1 INTRODUCTION

Onshore buried pipelines transporting oil and gas are vulnerable to seismically-induced permanent ground displacements, such as those resulting from seismic fault activation. Tectonic fault offset is the primary cause of earthquake-related catastrophic pipe failures [1]. The structural performance of buried pipes under faulting has drawn the attention of numerous researchers over the last decades, carrying out experimental, analytical, and numerical studies (e.g. [2]–[5]). However, in the vast majority of studies, fault offset is considered to be deterministic (i.e. a few rather arbitrary values are considered) or is estimated via empirical expressions that relate fault characteristics (e.g. earthquake magnitude, fault geometry, rupture length, etc.), such as those published by Wells and Coppersmith [6]. In the case of typical structures, such as building and bridges, numerous design codes, standards or guidelines are available to estimate the seismic loading for a predefined level of design hazard, typically as the result of probabilistic seismic hazard analysis. Contrarily, for buried pipelines, a single fault displacement magnitude is considered as the worst-case scenario, consisting of a postulated occurrence of an earthquake with a specific magnitude at a specific location. Consequently, pertinent uncertainties are disregarded, resulting in a hazard-independent estimation with an unknown level of conservatism.

The environmental, social, and economic repercussions of a potential pipeline failure call for the employment of state-of-the-art methods for the estimation of fault offset magnitude and therefore the design of pipelines at fault crossings. To achieve parity with the design standards for buildings and bridges, at the very least an approach is needed to set the design fault displacement for a pipeline at a pre-defined hazard level. Hence, a better balance between safety, capital/maintenance costs, and environmental responsibility can be attained. The appropriate such method is the Probabilistic Fault Displacement Hazard Analysis (PFDHA) that was introduced by Youngs et al. [7] for the seismic hazard assessment of the planned nuclear waste repository at Yucca Mountain, Nevada, USA.

Transmission and distribution pipelines form an extensive network, covering areas that range from a few hundred thousand square meters to entire countries. When seismic areas are traversed, crossing major or minor tectonic faults is almost inevitable. These faults might be active or inactive, or even not mapped due to inactivity during the last thousands of years. In case of crossing a major fault, this will be probably fully mapped and recorded, allowing the implementation of a full probabilistic hazard analysis (PFDHA) to account for all geotechnical and seismological parameters of the crossing. On the other hand, designers are aware that the latter is not the case for minor faults, typically being poorly mapped and recorded resulting in a minimum or even zero data availability. The problem is regularly treated based on a blend of expert opinion, engineering assumptions, and the implementation of empirical regression equations to calculate/estimate the design fault displacement. Thus, the aforementioned drawbacks of the deterministic approach are inflated again in the design. The present study stands as the first step to develop a set of simplified expressions for the estimation of fault offset magnitude for pipe – fault crossings, in case there is insufficient data. The expressions are derived from the statistical processing of PFDHA results taking into account typical values of the pertinent seismological parameters of the European area.

2 FAULT DISPLACEMENT HAZARD

2.1 Probabilistic Fault Displacement Hazard Analysis

The basis of Probabilistic Fault Displacement Hazard Analysis (PFDHA) was originally established by Youngs et al. [7] and later modified/improved, for example in [8]–[11]. The outcome of PFDHA is the mean annual frequency (MAF) of exceeding fault displacement levels

at a site by considering the fault geometry, the fault slip rate, the distribution of earthquakes, and the pertinent aleatory and epistemic uncertainties. PFDHA has been applied for the pipeline – fault crossing problem by the authors in [12], adopting the "earthquake approach" that is derived from the classic Probabilistic Seismic Hazard Analysis [13]. The "principal faulting" of PFDHA is considered under the assumption that the pipeline crosses a main fault, while distributed faulting issues are neglected. The fault displacement hazard estimation depends, among others, on the fault event rate, the maximum earthquake magnitude, the surface rupture length (SRL), the position of the rupture along the fault trace, and the position of the pipeline crossing site.

PFDHA for pipe – fault crossing site is essentially an application of the total probability theorem:

$$\lambda_D(d) = v \sum_i P(D > d|m_i) P_M(m_i) \tag{1}$$

where v is the mean annual rate (seismic rate) of all earthquakes above a minimum earthquake magnitude of engineering significance, following a Poisson model of occurrences, $P_M(m_i)$ is the probability of magnitude M falling within the i-th bin characterized by m_i at its center and is estimated using the Gutenberg-Richter bounded recurrence law [14]. $P(D>d|m_i)$ is the probability that the fault displacement D exceeds a defined value d at the crossing site, given an earthquake of magnitude m_i has occurred. Eq. (1) is applied for both the average fault displacement (AD) and the maximum fault displacement (MD) options of PFDHA, each one associated with a different fault displacement prediction equation, similar to a ground motion prediction equation of classic PSHA.

2.2 Hazard uncertainty

The identification and quantification of uncertainties is an integral part of seismic hazard analysis as the hazard curve is sensitive to the parameters adopted in the analysis. Any uncertainty can be incorporated in PFDHA. Uncertainties are classified into two main categories, namely aleatory and epistemic. Aleatory uncertainties are related to the inherent variability of nature, e.g. randomness in earthquake magnitude, fault displacement, etc., and are handled through sampling. Epistemic uncertainties are related to the incomplete understanding of nature and in time can be reduced with better observations, e.g. ground motion prediction equations. These uncertainties lead to alternative hazard curves and are handled through logic trees [15] by creating different models for input parameters and assigning weight factors to the tree branches. Weight factors represent the relative belief of the engineer in alternative models, without necessarily being frequency-based probabilities [16]. It is noted that there is no evidence (recorded data) for favoring the AD or MD approach of PFDHA. Thus, this option is considered as an epistemic uncertainty and is assigned a weight factor equal to 0.50 in a logic tree formulation.

3 METHODOLOGY OUTLINE

3.1 Parameters

The aforementioned formulation of fault displacement hazard estimation requires the following key input parameters:

- Seismic rate v of all earthquakes above magnitude 4.50 (minimum earthquake magnitude of engineering significance)
- Fault type (strike-slip, normal, reverse)

- Maximum earthquake magnitude (M_{max})
- b-value of the Gutenberg-Richter Bounded Recurrence Law [14] (slope of the curve)
- Fault length (LF) in km
- Pipe – fault crossing point (XL) that is the ration of the location of the crossing point to the closet fault edge to the fault length with $0 < XL \leq 0.50$

Specifically, the seismic rate according to Eq. (1) is an external multiplier of the seismic hazard calculations that are carried out separately for each fault type. On the other hand, for reasons of practicality, parameters M_{max}, b, FL, and XL are treated as discrete variables and are assigned indicative realistic values as per Table 1.

Parameter	Values
M_{max}	4.65, 5.00, 5.35, 5.65, 6.00, 6.35, 6.65, 7.00, 7.35, 7.75, 8.25
b	0.70, 0.90, 1.10
LF	10, 20, 50, 100, 150, 200
XL	0.10, 0.20, 0.30, 0.40, 0.50

Table 1: Parameters considered in fault displacement hazard estimation.

The range of b-values of the Gutenberg-Richter Bounded Recurrence Law [14] is from 0.70 to 1.10 for stable and active regions in Europe (EU SERA project, http://www.sera-eu.org/en/home/). The range of M_{max} values is 4.50 to 8.50, discretized in 11 bins with the bin centers listed in Table 1. Wells and Coppersmith [6] provide expressions that relate fault characteristics along with the pertinent limitations regarding the applicability of the expressions. Thus, in the case of normal/reverse fault, the maximum considered fault length (LF) is 100km (discretized in 4 values), while in the case of strike-slip fault it is 200km (discretized in 6 values).

3.2 Knowledge levels

Application of the full PFDHA framework, as described so far, necessitates seismological and geotechnical data that are not always available, for example, in case of minor faults or faults considered to be inactive. To account for input data incompleteness, the aim is to formulate pertinent expressions for the estimation of the design fault displacement for different levels of data availability, as presented indicatively in Table 2.

	Parameters				
Level	fault type	b	M_{max}	LF	XL
A	✓	✓	✓	✓	✓
B	✓			✓	✓
C				✓	✓
D / D1	✓			✓	
D / D2	✓		✓		
E / E1				✓	
E / E2			✓		

Table 2: Indicative levels of data knowledge for the pipeline – fault crossing site with reducing data availability from Level A to Level E.

The available data at each level reflects the objective difficulties in gathering all the necessary data. Assuming a minor fault, the length can be estimated by analyzing satellite images and determining then the fault crossing point. However, this fault might have been inactive for

a long period, and consequently estimating the maximum earthquake magnitude and the *b*-value of Gutenberg-Richter Law might not be possible.

The present study stands as the first step towards formulating simplified expressions for the estimation of the design fault displacement for pipelines crossing faults. The seismic rate v in Eq. (1) is assumed to be $v = 1$, reflecting areas of roughly moderate seismicity, namely areas where an earthquake of magnitude above 4.50 is expected once a year on average. Levels A and B of Table 2 are examined for all fault types, taking into account all the parameters of Table 1.

3.3 Design fault displacement

The typical return period of $T = 475$ yrs is considered in the current version of EN1998-4:2006 [17]. Structures of higher importance than the typical one (namely significance factor equal to one) are designed with seismic loads that are increased by multiplying with significance (or performance) factors higher than 1.00. More return periods and equivalent probabilities of exceedance (PoE) in 50 yrs are considered hereinafter (Table 3). In more detail, a return period of $T = 225$ yrs refers to low importance infrastructure (e.g., minor pipelines not carrying fuel), while $T = 975$ yrs and $T = 2475$ yrs are reserved for significant structures or infrastructure.

T	PoE in 50 yrs	MAF
225 yrs	20%	0.0045
475 yrs	10%	0.0021
975 yrs	5%	0.0010
2475 yrs	2%	0.0004

Table 3: Return periods (*T*) considered and equivalent probabilities of exceedance (PoE) in 50 yrs and corresponding mean annual frequencies (MAF).

4 LEVEL A

Level A of data knowledge is the one that requires all available data, namely fault type, *b*-value, magnitude M_{max}, fault length (*LF*), crossing point (*XL*). Considering all values of Table 1 for strike-slip, normal, and reverse fault type, PFDHA (section 2) is performed for all possible combinations of parameter values. In case of a strike-slip fault, the number of fault displacement hazard curves produced is equal to (11 values of M_{max}) × (3 *b*-values) × (6 values of *LF*) × (5 values of *XL*) = 990, while in case of normal and reverse fault the number of hazard curves is equal to (11 values of M_{max}) × (3 *b*-values) × (4 values of *LF*) × (5 values of *XL*) = 660. Then, to identify the effect of each parameter on the hazard curve, the case of normal faulting is examined in Figure 1 where in each case a single parameter is varied, while the other three are kept constant. The "anchoring" central set of parameter values for this example is $M_{max} = 6.65$, $b\text{-value} = 0.90$, $LF = 50\text{km}$, and $XL = 0.30$. The effect of maximum earthquake magnitude is evaluated in Figure 1(a), where for low fault offsets the range of MAFs is roughly from 10^{-3} to 10^{-2}, while for very high offsets this range is 10 times higher. In general, the increase of M_{max} leads to lower MAFs, indicating that a higher magnitude earthquake is rarer. Then, the effect of the Gutenberg-Richter *b*-value is examined in Figure 1(b), where the hazard curves for varying *b*-values are almost parallel to one another. The increase of the *b*-value leads to lower MAFs since the *b*-value is the slope of the curve that provides the "expected" future earthquake magnitude. Thus, a higher *b*-value implies that more low magnitude events "will occur" for each large magnitude event and consequently the overall rate of large magnitude events becomes lower.

The displayed behavior of the hazard curves for varying fault length in Figure 1(c) may seem peculiar, as longer faults may seem to underproduce small displacements. However, one should bear in mind that all curves are calculated for the same seismic rate $v = 1.00$ meaning that one event with magnitude $M \geq 4.50$ is expected on average per year. Thus, taking, for example, a small offset value of $d = 0.10\text{m}$, $\lambda(0.10\text{m}) = 0.0184$ for $LF = 10\text{km}$, while $\lambda(0.10\text{m}) = 0.0032$ for $LF = 100\text{km}$. The reason is that contrary to peak ground acceleration (PGA) or spectral acceleration $S_a(T_1)$ wave-propagation effects that affect points outside the immediate fault rupture, a fault offset cannot be recorded outside the rupture itself. Thus, on a longer fault, the many small events that could produce such a low value of $d = 0.10\text{m}$ actually happen away from the crossing point, reducing the corresponding MAF. When larger fault offsets are considered, larger magnitudes automatically come into play, rupturing larger segments of the fault to produce more frequent larger offsets. Thus, a fault length of 10km will very rarely produce a displacement of $d = 2\text{m}$, having a MAF of $\lambda \approx 10^{-5}$ versus a MAF of $\lambda \approx 1.5 \times 10^{-4}$ for the 100km fault.

Finally, the effect of the crossing point location along the fault trace is examined in Figure 1(d). Youngs et al. [7] used normalized fault displacement data for the estimation of the conditional probability that the offset at a specific point will exceed a predefined value. The normalization is expressed as D/AD or D/MD where D is the fault offset, AD is the average fault displacement, and MD is the maximum fault displacement. Distributions of ratios D/AD and D/DD are expressed as a function of the crossing point x/LF (XL) with $f(D/AD$ or $D/MD|x/LF)$ being symmetric about a maximum value at $x/L = 0.50$. Thus, higher fault displacement is expected for values x/LF close to 0.50, as presented in Figure 1(d), where hazard curves for higher x/LF are parallelly "displaced" to lower MAFs.

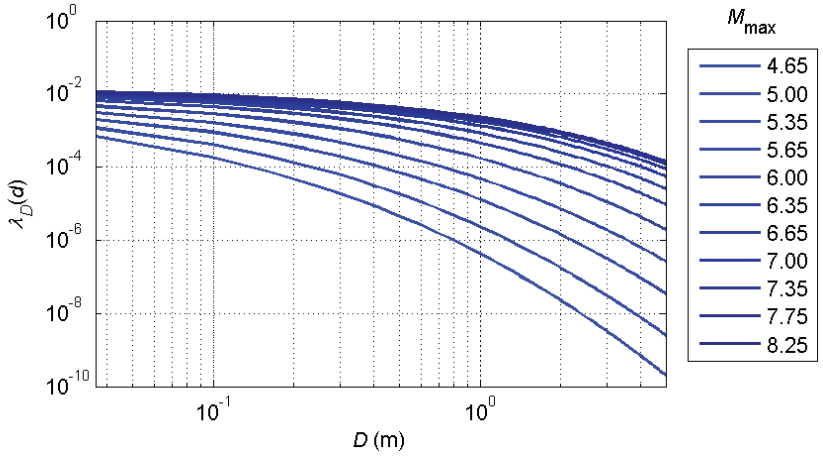

(a): varying magnitude M_{max}, b-value $= 0.90$, $LF = 50\text{km}$, and $XL = 0.30$

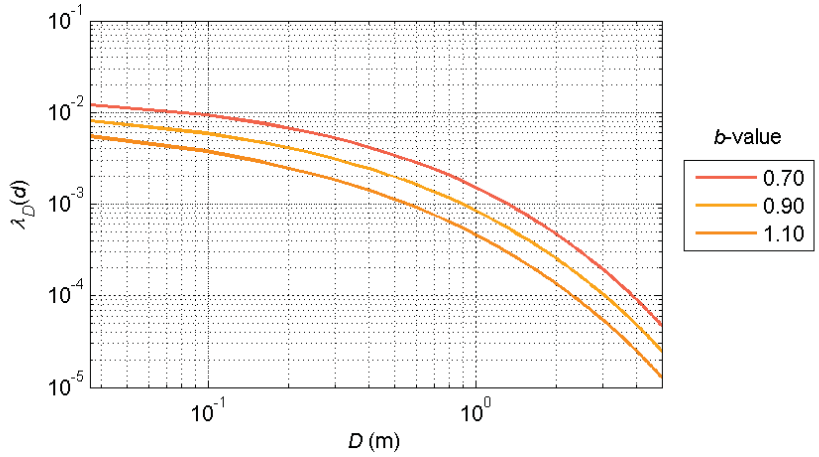

(b): $M_{\max} = 6.65$, varying b-value, $LF = 50$km, and $XL = 0.30$

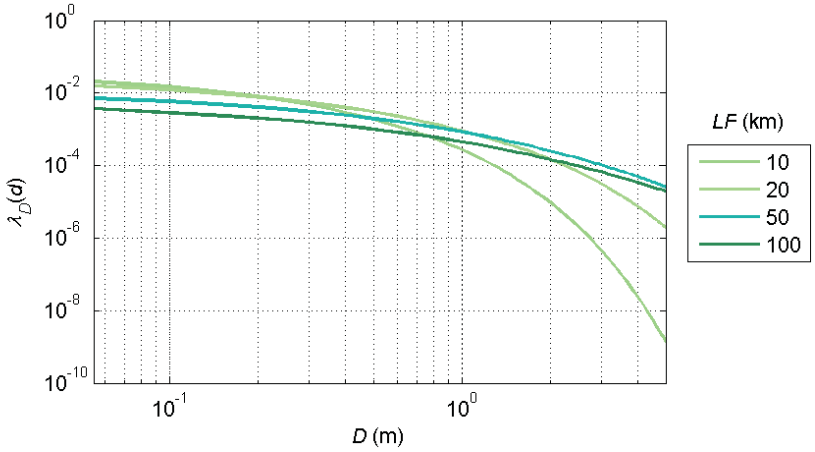

(c): $M_{\max} = 6.65$, b-value $= 0.90$, varying LF, and $XL = 0.30$

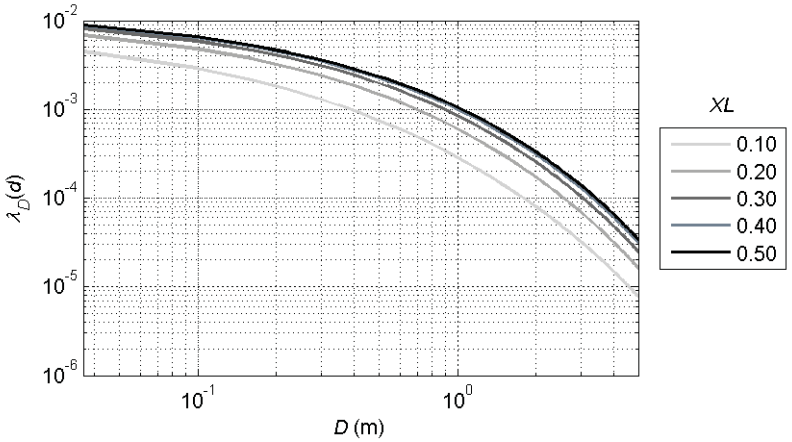

(d): $M_{\max} = 6.65$, b-value $= 0.90$, $LF = 50$km, and varying XL

Figure 1: Fault displacement hazard curves on pipeline crossing site.

5 LEVEL B

In knowledge Level B, the maximum earthquake magnitude ($M_{\max}$) and the b-value are unknown variables, as presented in Table 2. The logic tree of Figure 2 is formulated to handle the unknown variables by assigning pertinent weight factors to the tree branches. The weight factors for the b-value are listed in Table 4 and are selected based on expert opinion for European sites.

parameter value	weight factor w_b
0.70	0.1585
0.90	0.6830
1.10	0.1585

Table 4: Level B – weight factors for the parameter *b*-value of Gutenberg-Richter Law [14].

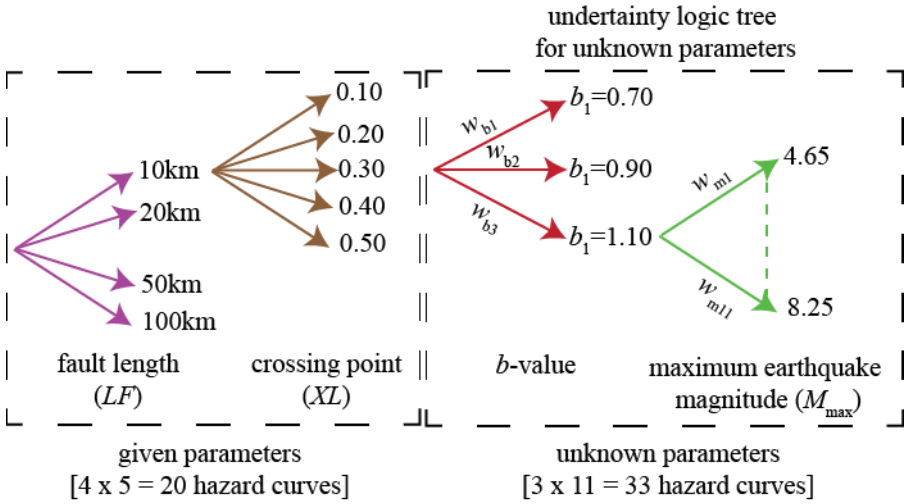

Figure 2: Logic tree formulation to handle unknown parameters in data knowledge Level B.

The weight factors for $M_{\max}$ are estimated based on the empirical expressions of Wells and Coppersmith [6]. The earthquake magnitude is normally distributed with respect to fault length (*LF*). The mean value of earthquake magnitude concerning *LF* and the corresponding standard deviation for each fault type are estimated after:

$$\text{Normal fault: } M_{mean} = 4.86 + 1.32\log_{10}(LF)\,,\sigma = 0.34 \tag{2}$$

$$\text{Reverse fault: } M_{mean} = 5.00 + 1.22\log_{10}(LF)\,,\sigma = 0.28 \tag{3}$$

$$\text{Strike-Slip fault: } M_{mean} = 5.16 + 1.12\log_{10}(LF)\,,\sigma = 0.28 \tag{4}$$

Thus, for every fault length considered, the mean earthquake magnitude is estimated using Eqs. (2)-(4). Then, the weight factor for each magnitude ($M_{\max}$) considered is evaluated as:

$$w_m = F(M_{\max}) = \Phi\left(\frac{M_{\max} - M_{mean}}{\sigma}\right) \tag{5}$$

In case of normal or reverse fault, following the procedure presented above along the logic tree of Figure 2 leads to the reduction of the total number of hazard curves (or combination of discrete parameter values) to consider from 660 to 20 [(4 values of *LF*) × (5 values of *XL*)], while in case of strike-slip fault the corresponding reduction is from 990 curves to 30 [(6 values of *LF*) × (5 values of *XL*)]. This reduction is simply achieved by summarizing the larger sample of hazard curves through the logic tree.

The next step in the process is to determine the fault offset values from each hazard curve that correspond to each return period of Table 3. The case of normal fault is illustrated in Figure 3, where the 20 hazard curves are plotted with solid lines and the 4 return periods under consideration are plotted with dashed horizontal lines. The grouping of hazard curves that is observed is related to the different fault lengths considered. In other words, the grouping of the

hazard curves is a combination of Figure 1(c) and Figure 1(d). The intersection of each horizontal line with a hazard curve provides a single point estimate of the fault offset, given the return period. Consequently, for each return period 20 fault offset values are estimated.

The fault displacement in meters with respect to fault length and crossing point can be estimated via the general function $d(LF, XL)$:

$$d(LF,XL) = p_{00} + p_{10}LF + p_{01}XL + p_{20}LF^2 + p_{11}(LF)(XL) + p_{02}XL^2 + p_{03}LF^3 + p_{21}(LF^2)(XL) + p_{12}(LF)(XL^2) \text{ (m)} \quad (6)$$

where p_{00}, p_{01}, …, p_{12} are the fitting coefficients. Evidently, to accommodate all observations on the relative significance of fault length (LF) and crossing point (XL), the length is captured with terms up to the third power, while for the crossing point, terms up to the second power are employed, including all interaction terms up to the third order. The resulting coefficients are listed in Table 5 for the normal fault, in Table 6 for the reverse fault, and in Table 7 for the strike-slip fault type. It is noted that Eq. (6) is applied for each return period of Table 3. Indicative results of the fitted surface for normal fault type and $T = 475$ yrs is shown in Figure 4. The root mean square error (RMSE), which is the standard deviation of the residuals (prediction errors), for each fitting is listed in Table 5 through Table 7, indicating that the error is at the order of a few centimeters, namely the data is very concentrated around the line of best fit. Finally, it is noted that the adjusted R-square is above 0.995 for all cases.

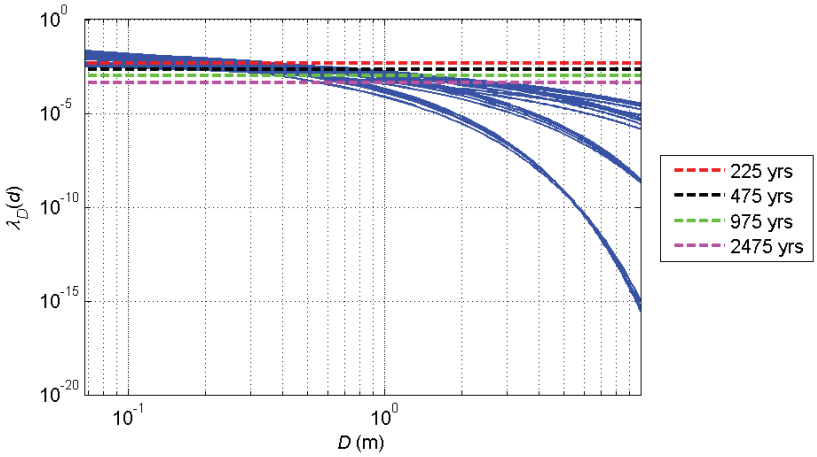

Figure 3: Normal fault: hazard curves (solid lines) of Level B and considered return periods (horizontal dashed lines).

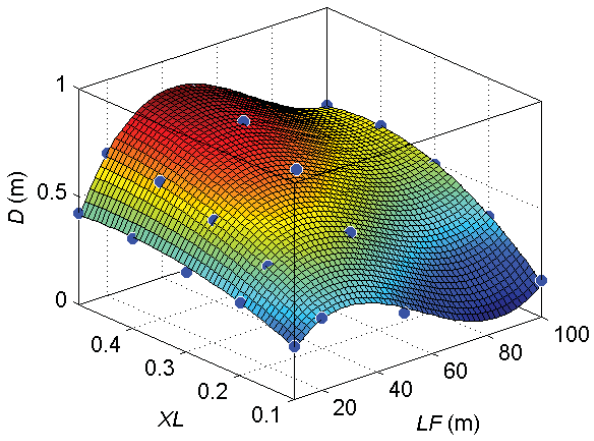

Figure 4: Normal fault: surface fitting for fault displacement values for $T = 475$ yrs.

Normal fault: coefficients for Eq. (6)											
T (yrs)	RMSE (m)	p_{00}	p_{10}	p_{01}	p_{20}	p_{11}	p_{02}	p_{30}	p_{21}	p_{12}	LF range (km)
225	0.007949	0.022940	0.008334	0.645058	-0.00031	0.029956	-0.84459	2.09E-06	-0.00021	-0.01306	10-100
475	0.014230	0.020385	0.015884	0.790144	-0.00049	0.064676	-1.39270	3.13E-06	-0.00041	-0.02287	10-100
975	0.022168	0.061270	0.024446	0.536158	-0.00066	0.113969	-1.30167	4.03E-06	-0.00054	-0.05946	10-100
2475	0.030221	0.111599	0.040342	-0.00829	-0.00090	0.181476	-0.78500	4.94E-06	-0.00061	-0.12243	10-100

Table 5: Normal fault: coefficients for estimating fault displacement in data knowledge Level B.

Reverse fault: coefficients for Eq. (6)											
T (yrs)	RMSE (m)	p_{00}	p_{10}	p_{01}	p_{20}	p_{11}	p_{02}	p_{30}	p_{21}	p_{12}	LF range (km)
225	0.011472	0.244408	-0.00727	1.731467	0	-0.00239	-1.66579	0	0	0	10-50
475	0.011735	0.369540	-0.00171	1.906638	-8.7E-05	0.008657	-1.55476	6.08E-07	-4.7E-05	-0.01238	10-100
975	0.018966	0.472529	0.00565	2.121767	-0.00020	0.017519	-1.41466	1.18E-06	-6.0E-05	-0.02203	10-100
2475	0.031966	0.645046	0.01593	2.063252	-0.00037	0.037789	-0.52237	2.04E-06	-6.7E-05	-0.04999	10-100

Table 6: Reverse fault: coefficients for estimating fault displacement in data knowledge Level B.

Strike-Slip fault: coefficients for Eq. (6)											
T (yrs)	RMSE (m)	p_{00}	p_{10}	p_{01}	p_{20}	p_{11}	p_{02}	p_{30}	p_{21}	p_{12}	LF range (km)
225	0.008359	0.013616	0.002373	0.653752	-6.8E-05	0.004795	-0.79558	0	0	0	10-50
475	0.027420	-0.001060	0.004466	0.868048	-8.1E-05	0.020072	-1.02385	2.68E-07	-7.5E-05	-0.00689	10-200
975	0.034403	-0.023590	0.007158	1.229490	-0.00010	0.047720	-1.86840	3.14E-07	-0.00013	-0.01972	10-200
2475	0.034899	0.076041	0.012777	0.593121	-0.00015	0.099034	-1.18712	3.77E-07	-0.00014	-0.07030	10-200

Table 7: Strike-slip fault: coefficients for estimating fault displacement in data knowledge Level B.

6 CONCLUSIONS

The estimation of design fault displacement for buried pipelines crossing active tectonic faults typically relies on regression equations, engineering assumptions, or expert opinion. Pipelines are structures of very high importance and consequently, it is deemed necessary to employ state-of-the-art probabilistic tools for the estimation of the design fault displacement. However, pipelines extend over hundreds or thousands of kilometers, crossing several major or minor, active, or potentially inactive tectonic faults. Thus, performing a full probabilistic hazard assessment of each fault crossing might not be possible or even desirable. Therefore, we presented a comprehensive first attempt to formulate simplified expressions for the calculation of the fault displacement.

The appropriate method for the seismic hazard assessment of fault is the Probabilistic Fault Displacement Hazard Analysis (PFDHA) that has been adjusted by the authors for buried pipeline – fault crossings. Considering a range of realistic values for the key input parameters of PFDHA, namely fault type, maximum earthquake magnitude, fault length, crossing point, and *b*-value for earthquake magnitude recurrence, analysis is carried out for all combinations of the input parameters. Results are then statistically processed by taking into account reduced levels of data knowledge, namely unknown parameters, to formulate simplified expressions that relate fault characteristics and fault offset, given the desired return period.

The developed simplified expressions are the first decisive step towards formulating a methodology for estimating the design fault displacement for pipeline – fault crossing considering different knowledge levels and with respect to the required return period. The proposed methodology aims at overcoming the typical drawbacks of the deterministic approach (regression equations, expert opinion, etc.), where pertinent uncertainties are disregarded, resulting in a hazard-independent estimation with an unknown level of conservatism.

7 ACKNOWLEDGMENTS

This research received funding from the European Union's HORIZON 2020 research and innovation programme under grant agreement No 821054, project: "HYPERION – Development of a Decision Support System for Improved Resilience & Sustainable Reconstruction of historic areas to cope with Climate Change & Extreme Events based on Novel Sensors and Modelling tools".

REFERENCES

[1] M.J. O'Rourke, J.X. Liu, *Seismic Design of Buried and Offshore Pipelines. Monograph MCEER-12-MN04*, Multidisciplinary Center for Earthquake Engineering Research, 2012.

[2] G.C. Sarvanis, S.A. Karamanos, Analytical model for the strain analysis of continuous buried pipelines in geohazard areas, *Engineering Structures* 152, 57-69, 2017.

[3] F.R. Rofooei, N.K.A. Attari, H.H. Jalali, New method of modeling the behavior of buried steel distribution pipes subjected to reverse faulting, *Journal of Pipeline Systems Engineering and Practice* 9(1), 1-13, 2018.

[4] H.E. Demirci, S. Bhattacharya, D. Karamitros, N. Alexander, Experimental and numerical modelling of buried pipelines crossing reverse faults, *Soil Dynamics and Earthquake Engineering* 114, 198-214, 2018.

[5] A. Tsatsis, M. Loli, G. Gazetas, Pipeline in dense sand subjected to tectonic deformation from normal or reverse faulting, *Soil Dynamics and Earthquake Engineering* 127, 105780, 2019.

[6] D.L. Wells, K.J. Coppersmith, New empirical relationships among magnitude, rupture length, rupture width, rupture area, and surface displacements, *Bulletin of the Seismological Society of America* 84(4), 974-1002, 1994.

[7] R.R. Youngs *et al.*, A methodology for probabilistic fault displacement hazard analysis (PFDHA), *Earthquake Spectra* 19(1), 191-219, 2003.

[8] R.E.S. Moss, Z.E. Ross, Probabilistic fault displacement hazard analysis for reverse faults, *Bulletin of the Seismological Society of America* 101(4), 542-1553, 2011.

[9] M.M. Angell, A.O.A. Geophysics, K. Hanson, R.R. Youngs, H. Abramson, Probabilistic fault displacement hazard assessment for flowlines and export pipelines, mad dog and Atlantis field developments, deepwater Gulf of Mexico, *Proceedings of the Annual Offshore Technology Conference*, 2579-2603, 2003.

[10] M.D. Petersen *et al.*, Fault displacement hazard for strike-slip faults, *Bulletin of the Seismological Society of America* 101(2), 805-825, 2011.

[11] R. Chen, M. D. Petersen, Probabilistic fault displacement hazards for the Southern San Andreas fault using scenarios and empirical slips, *Earthquake Spectra* 27(2), 293-313, 2011.

[12] V.E. Melissianos, D. Vamvatsikos, C.J. Gantes, Performance Assessment of Buried Pipelines at Fault Crossings, *Earthquake Spectra* 33(1), 201-218, 2017.

[13] C.A. Cornell, Engineering seismic risk analysis, *Bulletin of the Seismological Society of America* 58(5), 1583-1606, 1968.

[14] R. Gutenberg, C.F. Richter, Frequency of earthquakes in California, *Bulletin of the Seismological Society of America* 34, 185-188, 1944.

[15] J.J. Bommer, F. Scherbaum, The use and misuse of logic trees in probabilistic seismic hazard analysis, *Earthquake Spectra 2*4(4), 997-1009, 2008.

[16] N.A. Abrahamson, J.J. Bommer, Probability and uncertainty in seismic hazard analysis, *Earthquake Spectra* 21(2), 603-607, 2005.

[17] European Committee for Standardization (CEN), *EN 1998-4:2006, Eurocode 8 - Design of structures for earthquake resistance - Part 4: Silos, tanks and pipelines*, 2006.